AD-A127 245   ADAPTIVE ARRAY BEHAVIOR WITH PERIODIC ENVELOPE   1/1
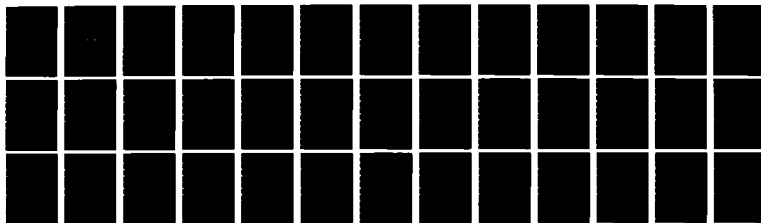MODULATED INTERFERENCE(U) OHIO STATE UNIV COLUMBUS
ELECTROSCIENCE LAB   A S AL-RUWAIS ET AL. DEC 82
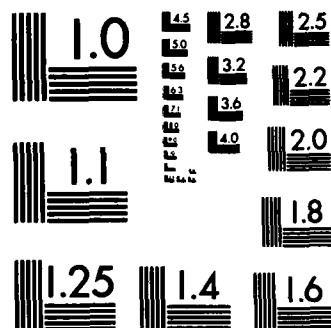
UNCLASSIFIED   ESL-714505-1 N00019-82-C-0190   F/G 9/5   NL

MICROCOPY RESOLUTION TEST CHART

NATIONAL BUREAU OF STANDARDS-1963-A

OSU

The Ohio State University

ADAPTIVE ARRAY BEHAVIOR WITH PERIODIC ENVELOPE

MODULATED INTERFERENCE

A.S. Al-Ruwais
R.T. Compton, Jr.

The Ohio State University
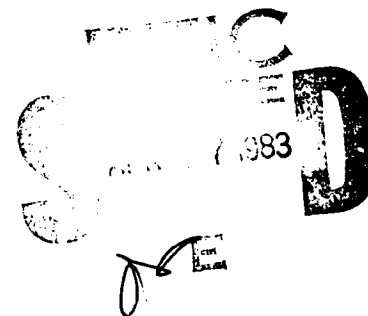
ElectroScience Laboratory

Department of Electrical Engineering
Columbus, Ohio 43212

DTIC FILE COPY

83 04 26 008

NOTICES

When Government drawings, specifications, or other data are used for any purpose other than in connection with a definitely related Government procurement operation, the United States Government thereby incurs no responsibility nor any obligation whatsoever, and the fact that the Government may have formulated, furnished, or in any way supplied the said drawings, specifications, or other data, is not to be regarded by implication or otherwise as in any manner licensing the holder or any other person or corporation, or conveying any rights or permission to manufacture, use, or sell any patented invention that may in any way be related thereto.

50272-101

REPORT DOCUMENTATION PAGE	1. REPORT NO.		A127245	3. Recipient's Accession No

4. Title and Subtitle		5. Report Date
ADAPTIVE ARRAY BEHAVIOR WITH PERIODIC ENVELOPE MODULATED INTERFERENCE		December 1982
		6.

7. Author(s)	8. Performing Organization Rept. No.
A.S. Al-Ruwais and R.T. Compton, Jr.	ESL 714505-1

9. Performing Organization Name and Address	10. Project/Task/Work Unit No.
The Ohio State University ElectroScience Laboratory Department of Electrical Engineering Columbus, Ohio 43212	11. Contract(C) or Grant(G) No
	(C)
	(G) N00019-82-C-0190

12. Sponsoring Organization Name and Address	13. Type of Report & Period Covered
Naval Air Systems Command Washington, D.C. 20361	Technical Report
	14.

15. Supplementary Notes

The authors (first page, 1941)

16. Abstract (Limit: 200 words)

We present a method for determining the effects of envelope modulated interference on an LMS adaptive array. The interference is assumed to have periodic envelope modulation with a bandwidth small compared to the carrier frequency. For such interference, the method allows one to calculate the periodic steady-state behavior of the array weights and the resulting array performance.

As an example, we compute the effects of an ordinary amplitude modulated (AM) interference signal on the array. It is shown that such interference causes the array to modulate the desired signal envelope but not its phase. With a DPSK desired signal, AM interference is found to have about the same effect on bit error probability as CW interference.

computed are

17. Document Analysis a. Descriptors

b. Identifiers/Open-Ended Terms

c. COSATI Field/Group

18. Availability Statement	19. Security Class (This Report)	21. No. of Pages
APPROVED FOR PUBLIC RELEASE DISTRIBUTION UNLIMITED	Unclassified	33
	20. Security Class (This Page)	22. Price
	Unclassified	

(See ANSI–Z39.18)   See Instructions on Reverse   OPTIONAL FORM 272 (4-77)
(Formerly NTIS–35)
Department of Commerce

i

TABLE OF CONTENTS

Page

Accession For

NTIS GRA&I	☒
DTIC TAB	☐
Unannounced	☐
Justification	

By
Distribution/
Availability Codes
Avail and/or
Dist   Special

A

iii

LIST OF FIGURES

FIGURE   Page

v

I. INTRODUCTION

The performance of an LMS (Least Mean Square) adaptive array [1] can be different with modulated interference than with single frequency (CW) interference. Under certain conditions, interference modulated at a rate slow enough to be tracked by the array feedback can cause the weights to vary continuously and prevent them from reaching steady-state. In this situation the output signal-to-interference-plus-noise ratio (SINR) from the array varies continuously and the array modulates the desired signal.

Pulsed interference is a simple example of modulated interference. The effect of a pulsed interference signal on an adaptive array has been described in [2]. It was shown, for example, that when the array receives a differential phase-shift keyed (DPSK) communication signal, pulsed interference increases the bit error probability more than CW interference for certain choices of the signal parameters.

The behavior of an LMS array has also been described for a double-sideband, suppressed carrier, amplitude modulated (DSBSC-AM) interference signal[3]. This special modulation was studied because it results in a differential equation for the array weights that can be solved. (Arbitrary types of interference modulation lead to an intractable mathematical problem.) For DSBSC-AM interference, the array weights satisfy a vector differential equation with properties similar

1

to the classical Mathieu equation [4]. By using an approach similar to the classical technique, it is possible to obtain the complete behavior of the array weights for this type of interference. It was shown in [3] that DSBSC-AM interference can cause the array to modulate the desired signal envelope, but that its effect on bit error probability with a DPSK signal is not much different than that of CW interference.

The purpose of the present report is to extend the technique used in [3] to handle interference with more general types of envelope modulation. The technique we present here requires that the interference have only envelope modulation (i.e., no phase modulation) and that the interference modulation be periodic. Also, it must be possible to approximate the interference modulation with a finite number of Fourier Series terms. In principle the number of terms used can be any finite number, but in practice the computational effort increases with the number of terms.

To illustrate the use of this method, we examine the LMS array performance with a simple amplitude modulated (AM) interference signal (a carrier and two sidebands). In general, this interference has the same effects on array performance as pulsed and DSBSC-AM interference: it causes the array output SINR to vary with time, and it produces envelope modulation, but not phase modulation, on the desired signal.

Section II of the report presents a method that can be used to determine the array weights and evaluate the array performance for an interference signal with arbitrary periodic envelope modulation. Section III presents calculated results obtained with this method for an AM interference signal. Section IV contains the conclusions.

II. FORMULATION OF THE PROBLEM

Consider an adaptive array with three isotropic elements a half wavelength apart, as shown in Figure 1. The analytic signal $\tilde{x}_j(t)$ from element j is multiplied by complex weight w_j and summed to produce the array output $\tilde{s}(t)$. The error signal $\tilde{\epsilon}(t)$ is the difference between the reference signal $\tilde{r}(t)$ and the array output $\tilde{s}(t)$. The array weights are contolled by LMS feedback loops [1,5] and satisfy the system of equations

$$\frac{dW}{dt} + k\Phi W = kS \tag{1}$$

where $W = (w_1, w_2, w_3)^T$ is the weight vector, Φ is the covariance matrix,

$$\Phi = E(X^* X^T) \tag{2}$$

S is the reference correlation vector,

$$S = E[X^* \tilde{r}(t)], \tag{3}$$

3

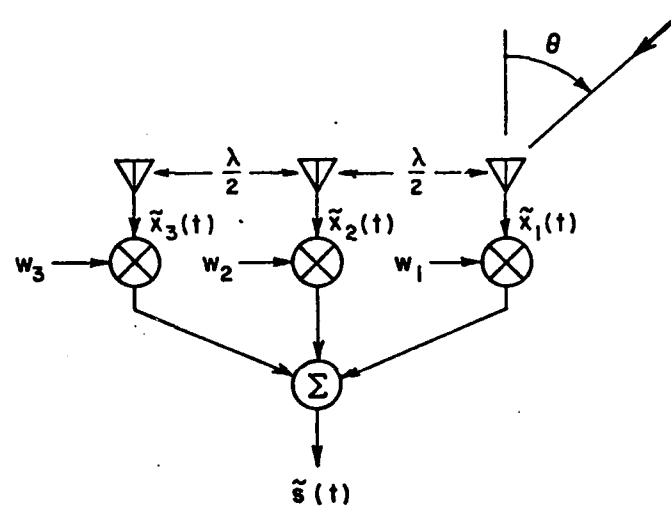Figure 1.   A Three-Element LMS Aray.

and k is the LMS loop gain. In these equations, X is the signal vector,

$$X = [\tilde{x}_1(t), \tilde{x}_2(t), \tilde{x}_3(t)]^T, \tag{4}$$

T denotes transpose, * complex conjugate, and $E[\cdot]$ expectation.

We assume that a desired and an interference signal are incident on the array and that thermal noise is also present in each element signal. The signal vector then contains three terms,

$$X = X_d + X_i + X_n, \tag{5.}$$

where X_d, X_i and X_n are the desired, interference and thermal noise vectors, respectively.

We assume the desired signal is CW and incident from angle θ_d relative to broadside. (θ is defined in Figure 1.) The desired signal vector is then

$$X_d = A_d e^{j(\omega_0 t + \psi_d)} U_d \quad , \tag{6}$$

where A_d is the amplitude, ω_0 is the carrier frequency, ψ_d is the carrier phase angle, and U_d is a vector containing the interelement phase shifts,

$$U_d = (1, e^{-j\phi_d}, e^{-j2\phi_d})^T \quad , \tag{7}$$

with

$$\phi_d = \pi\sin\theta_d . \tag{8}$$

5

We assume ψ_d is a random variable uniformly distributed on $(0, 2\pi)$.

Next, we assume an envelope modulated interference signal, as shown in Figure 2, arriving from angle θ_i. The interference signal vector is

$$X_i = A_i e^{j(\omega_0 t + \psi_i)} \begin{pmatrix} a_i(t) \\ a_i(t-T_i)e^{-j\omega_0 T_i} \\ a_i(t-2T_i)e^{-j2\omega_0 T_i} \end{pmatrix} \qquad (9)$$

where A_i is the amplitude, $a_i(t)$ is the envelope modulation received on element 1, ψ_i is the carrier phase angle, and T_i is the interelement time delay,

$$T_i = \frac{\pi}{\omega_0} \sin \theta_i \qquad (10)$$

We assume ψ_i is a random variable uniformly distributed on $(0, 2\pi)$ and statistically independent of ψ_d.

We assume the modulation envelope $a_i(t)$ is a periodic waveform. To make the definitions of $a_i(t)$ and A_i unique, we assume $a_i(t)$ has a peak value of unity during the period:

$$\max_{0 < t < T} a_i(t) = 1 \qquad (11)$$

where T is the period of $a_i(t)$. With this normalization, A_i^2 is the peak interference power per array element. In addition, we assume the rate
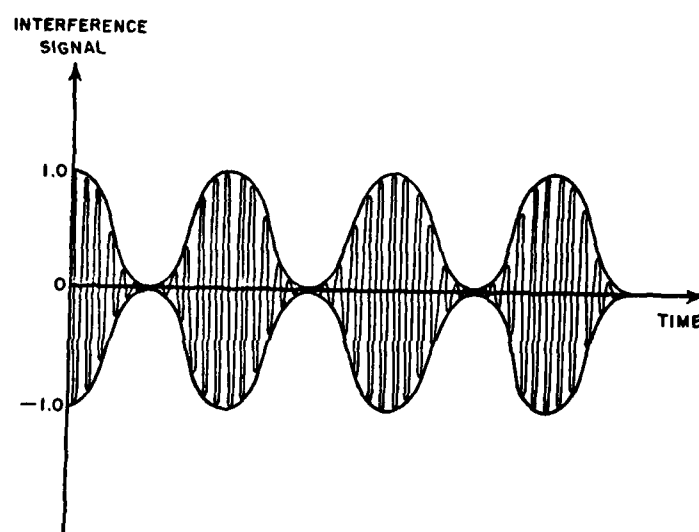
6

Figure 2. <u>AM Interference.</u>

of change of $a_i(t)$ is small enough that $a_i(t)$ changes only a negligible amount during the propagation time $2T_i$ across the array. (Or, equivalently, we assume that the bandwidth of $a_i(t)$ is very small compared to the carrier frequency ω_0.) Under this condition, the modulation envelopes in (9) are all essentially the same,

$$a_i(t) \simeq a_i(t-T_i) \simeq a_i(t-2T_i) \tag{12}$$

so (9) may be written

$$X_i = A_i a_i(t)e^{j(\omega_0 t+\psi_i)}U_i \tag{13}$$

where

$$U_i = (1, e^{-j\phi_i}, e^{-j2\phi_i}) \tag{14}$$

with

$$\phi_i = \omega_0 Ti = \pi\sin\theta_i \quad . \tag{15}$$

Finally, we assume the thermal noise vector is given by

$$X_n = [\tilde{n}_1(t), \tilde{n}_2(t), \tilde{n}_3(t)]^T , \tag{16}$$

where the $\tilde{n}_j(t)$ are zero-mean, gaussian thermal noise voltages, all statistically independent of each other and of ψ_d and ψ_i, and each of power σ^2. Thus,

$$E[\tilde{n}_j{}^*(t)\tilde{n}_k(t)] = \sigma^2\delta_{jk} , \tag{17}$$

8

Under these assumptions, the covariance matrix in (2) becomes

$$\Phi = \Phi_d + \Phi_i + \Phi_n \, , \tag{18}$$

with

$$\Phi_d = A_d^2 U_d^* U_d^T \tag{19}$$

$$\Phi_i = A_i^2 a_i^2(t) U_i^* U_i^T \tag{20}$$

and

$$\Phi_n = \sigma^2 I, \tag{21}$$

where I is the identity matrix.

To compute the reference correlation vector S in (3), the reference signal $\tilde{r}(t)$ must first be defined. In practice, the reference signal is usually derived from the array output [6-8]. It must be a signal correlated with the desired signal and uncorrelated with the interference. Here we assume the reference signal to be a replica of the desired signal,

$$\tilde{r}(t) = A_r e^{j(\omega_0 t + \psi_d)} . \tag{22}$$

Equation (3) then yields

$$S = A_r A_d U_d^* . \tag{23}$$

Equations (18)-(21) and (23) can now be inserted into (1) to give the differential equation for the weight vector W,

9

$$\frac{dW}{dt} = k[\sigma^2 I + A_d^2 U_d^* U_d^T + A_i^2 a_i^2(t) U_i^* U_i^T] W(t) = kA_r A_d U_d^* \quad . \tag{24}$$

Before solving (24) we put it in normalized form. First, dividing by $k\sigma^2$ gives

$$\frac{dW(t')}{dt'} + [I + \xi_d U_d^* U_d^T + \xi_i a_i^2(t') U_i^* U_i^T] W(t') = \frac{A_r}{\sigma} \sqrt{\xi_d} U_d^* \tag{25}$$

where

$$\xi_d = \frac{A_d^2}{\sigma^2} = \text{input signal-to-noise ratio (SNR) per element.}$$

$$\xi_i = \frac{A_i^2}{\sigma^2} = \text{peak input interference-to-noise ratio (INR) per element,}$$

and where we have also used a normalized time variable,

$$t' = k\sigma^2 t = \text{normalized time.}$$

Next, we note that the constant A_r/σ on the right side of (25) will just appear as a scale factor in the solution for W. It has no effect on the array output signal-to-noise ratios to be computed below. Hence, we arbitrarily set $A_r/\sigma=1$ to eliminate it. Finally, by defining

$$\Phi_1 = I + \xi_d U_d^* U_d^T \quad , \tag{26}$$

Equation (25) may be written

$$\frac{dW(t')}{dt'} + [\Phi_1 + \xi_i a_i^2(t')U_i^* U_i^T]W(t') = \xi_d U_d^* . \tag{27}$$

Since we assumed $a_i(t)$ to be a periodic waveform, $a_i^2(t')$ is also periodic and may be expanded in a Fourier series:

$$a_i^2(t') = \sum_{\ell=-\infty}^{\infty} P_\ell e^{j\ell\omega_m' t'} \tag{28}$$

where the P_ℓ are the Fourier coefficients and ω_m' is the normalized fundamental frequency of $a_i(t')$. (ω_m' is equal to $\omega_m/k\sigma^2$, where ω_m is the fundamental frequency of $a_i(t)$.) As discussed above, $a_i(t)$ is assumed to have a bandwidth small compared with the carrier frequency ω_0. In particular, we shall assume that only a finite number of coefficients in (28) are nonzero, i.e., that $P_\ell = 0$ for all $|\ell| > L$, where L is some integer. Equation (28) is then

$$a_i^2(t') = \sum_{\ell=-L}^{L} P_\ell e^{j\ell\omega_m' t'} . \tag{29}$$

Equation (27) is a linear vector differential equation with a constant source term on the right but with periodic time-varying coefficients. As has been discussed by D'Angelo [9], the solution for $W(t')$ will be a periodic function of time after the initial transients have died out. In this report, we do not consider the initial transients. We concentrate on the periodic steady-state solution for

11

$W(t')$. Once any initial transients have ended, $W(t')$ can be represented by a Fourier Series,

$$W(t') = \sum_{n=-\infty}^{\infty} C_n e^{jn\omega_m't'} \tag{30}$$

where C_n is a vector Fourier coefficient. Substituting (29) and (30) into (27) and collecting terms with the same frequency, we find that the coefficients C_n must satisfy

$$(jn\omega_m'I+\Phi_1) C_n + \xi_i U_i^* U_i^T \sum_{\ell=-L}^{L} P_\ell C_{n-\ell} = \sqrt{\xi_d}\ U_d^*\ \delta_{no}, \quad -\infty < n < \infty \ . \tag{31}$$

This equation may be solved for the C_n by expressing each C_n in terms of its components parallel and perpendicular to the vector U_i^*. To do this, we form a set of three orthonormal basis vectors* e_k

$$e_j^\dagger e_k = \delta_{jk} \ , \quad 1 < j. \ k < 3 \ , \tag{32}$$

(where $\dagger$ is conjugate transpose). We let e_1 be a unit vector parallel to U_i^*:

$$e_1 = \frac{U_i^*}{\sqrt{U_i^T U_i^*}} \ . \tag{33}$$

---

*The array has 3 elements, so $W(t')$ and C_n each have 3 components. Three basis vectors are needed to span the space for C_n.

We let e_2 be perpendicular to e_1 and lie in the plane defined by U_d^* and U_i^*:

$$e_2 = \zeta[U_d^* - \kappa U_i^*] \tag{34}$$

where ζ and κ are constants. Enforcing the orthonormality condition (32) yields

$$\kappa = \frac{U_i^T U_d^*}{U_i^T U_i^*} \tag{35}$$

and

$$\zeta = \left(U_d^T U_d^* - \frac{|U_i^T U_d^*|^2}{U_i^T U_i^*} \right)^{-1/2} . \tag{36}$$

The third vector e_3 can readily be found from e_1 and e_2 but will not be needed below, so we shall not compute it explicitly.

Each coefficient C_n may be written in terms of the unit vectors e_k as

$$C_n = \sum_{k=1}^{3} \alpha_{n,k} e_k \tag{37}$$

where the $\alpha_{n,k}$ are scalar coefficients. $\alpha_{n,k}$ is the component of C_n along the unit vector e_k.

13

Substituting (37) into (31) and multiplying the result on the left by $e_p^\dagger$ (for $p = 1, 2$ or 3) gives

$$jn\omega_m' \sum_{k=1}^{3} \alpha_{n,k} \, \delta_{pk} + \sum_{k=1}^{3} \alpha_{n,k} \, f_{pk}$$

$$+ \, \xi_i (e_p^\dagger U_i^*) \sum_{\ell=-L}^{L} P_\ell \sum_{k=1}^{3} \alpha_{n-\ell,k} \, (U_i^T e_k)$$

$$= \sqrt{\xi_d} \, (e_p^\dagger U_d^*) \, \delta_{no} \quad , \tag{38}$$

where

$$f_{pk} = e_p^\dagger \phi_1 e_k \quad . \tag{39}$$

The values of the f_{pk} may be found from (26) and (32) - (36). The result is

$$f_{11} = 1 + \xi_d \, \frac{|U_i^T U_d^*|^2}{U_i^T U_i^*} \quad , \tag{40}$$

$$f_{22} = 1 + \frac{\xi_d}{\zeta^2} \, , \tag{41}$$

$$f_{12} = f_{21}^* = \frac{\xi_d}{\zeta} \, \frac{U_i^T U_d^*}{\sqrt{U_i^T U_i^*}} \quad , \tag{42}$$

14

$$f_{13} = f_{31} = f_{23} = f_{32} = 0 \quad, \tag{43}$$

and

$$f_{33} = 1 \quad . \tag{44}$$

To determine the $\alpha_{n,k}$, we proceed as follows. First, since $e_3^\dagger U_i^* = e_3^\dagger U_d^* = 0$, applying (38) for $p = 3$ gives

$$\alpha_{n,3} = 0 \quad, \quad -\infty < n < \infty \quad . \tag{45}$$

Then, since $e_2^\dagger U_i^* = 0$, applying (38) for $p = 2$ and rearranging gives

$$\alpha_{n,2} = \frac{\sqrt{\xi_d}\,(e_2^\dagger U_d^*)\delta_{no} - \alpha_{n,1}f_{21}}{jn\omega_m' + f_{22}} \quad . \tag{46}$$

This equation allows us to calculate the $\alpha_{n,2}$ from $\alpha_{n,1}$. Hence, the problem of determining $W(t')$ is reduced to the problem of finding the $\alpha_{n,1}$.

To obtain the $\alpha_{n,1}$, we apply (38) for $p = 1$ and use (46) to substitute for $\alpha_{n,2}$. This process yields the following relation between the $\alpha_{n,1}$:

$$h_n \; \alpha_{n,1} + \sum_{\ell=-L}^{L} P_\ell \; \alpha_{n-\ell,1} = C \; \delta_{no} \tag{47}$$

where

$$h_n = \frac{(f_{11}+jn\omega_m')(f_{22}+jn\omega_m') - |f_{12}|^2}{\xi_i(f_{22}+jn\omega_m')|U_i^*|^2} \tag{48}$$

and

$$C = \frac{\sqrt{\xi_d}}{\xi_i|U_i^*|^2}\left(e_1^\dagger - \frac{f_{12}}{f_{22}} e_2^\dagger\right) U_d^* \quad . \tag{49}$$

Equation (47) holds for each value of n and is a 2L+1 term
recursion relation between the $\alpha_{n,1}$. If the values of $\alpha_{n,1}$ were known
for 2L successive terms, one could find all the other $\alpha_{n,1}$ from (47).
However, if one starts with an arbitrary initial set of 2L terms, the
$\alpha_{n,1}$ will not converge. Since the solution for W(t') in (30) must
converge, the $\alpha_{n,1}$ must approach zero as $n\to\pm\infty$. To obtain a solution for
W(t'), we therefore use the following method. We assume that there is
some N such that for all $|n|>N$, the $\alpha_{n,1}$ are essentially zero, i.e., we
assume that W(t') in (30) can be adequately approximated by a finite
sum

$$W(t') = \sum_{n=-N}^{N} C_n e^{jn\omega_m't} \quad . \tag{50}$$

16

If the $\alpha_{n,1}$ are zero for $|n| > N$, then the recursion relation (47) reduces to the finite system of equations,

$$
\begin{bmatrix}
h_N + P_o & P_1 \cdots \cdots P_L & 0 \cdots \cdots 0 \cdots 0 \\
P_{-1} & h_{N-1} + P_o & P_1 \cdots P_L \cdots \cdots 0 \cdots 0 \\
\vdots & \vdots & \vdots & \vdots \\
0 \cdots \cdots 0 & P_{-L} \cdots P_{-1} & h_o + P_o \ P_1 \cdots P_L & 0 \cdots 0 \\
\vdots & \vdots & & \vdots \\
0 \cdots \cdots 0 \cdots 0 & P_{-L} \cdots \cdots \cdots P_{-1} & h_{-N} + P_o
\end{bmatrix}
\begin{bmatrix}
\alpha_{N,1} \\
\alpha_{N-1,1} \\
\vdots \\
\alpha_{0,1} \\
\vdots \\
\alpha_{-N,1}
\end{bmatrix}
=
\begin{bmatrix}
0 \\
0 \\
\vdots \\
C \\
\vdots \\
0
\end{bmatrix}
$$

(51)

The nonzero $\alpha_{n,1}$ can be found by solving (51) numerically.

For this approach to yield accurate results, N must in fact be large enough that at least 2L of the $\alpha_{n,1}$ are essentially zero on each end of the $\alpha_{n,1}$ vector in (51). If this vector has 2L zeros on each end, the solution obtained from (51) will be the same as the solution of the infinite system in (47). In practice, a suitable value of N may be determined by increasing N until the $\alpha_{n,1}$ vector has 2L terms on each

17

end that are essentially zero. Experience in specific cases quickly shows how large N must be. Once the $\alpha_{n,1}$ are determined, the $\alpha_{n,2}$ may be found from (46). From $\alpha_{n,1}$ and $\alpha_{n,2}$ (and $\alpha_{n,3}=0$), the C_n may be evaluated from (37) and $W(t')$ from (30).

The time-varying weights in (30) have two effects on array performance. First, they cause the array to modulate the desired signal. (The array becomes a time-varying, or frequency dispersive, channel [10]). Second, the array output signal-to-interference-plus-noise ratio (SINR) varies periodically with time.

Given a time-varying weight vector $W(t')$, the desired signal component of the array output is

$$\tilde{s}_d(t') = A_d W^T(t') U_d e^{j(\omega_0' t' + \psi_d)} \quad , \tag{52}$$

(where $\omega_0' = \omega_0/k\sigma^2$). To study the modulation on $\tilde{s}_d(t)$, we define

$$a_d(t') e^{j\eta_d(t')} = A_d W^T(t') U_d \; . \tag{53}$$

Then $a_d(t') = A_d|W^T(t')U_d|$ is the envelope modulation and $\eta_d(t') = \angle W^T(t')U_d$ is the phase modulation. Furthermore, we define $a_{dn}(t')$ to be the envelope normalized to its value in the absence of interference, i.e.,

18

$$a_{dn}(t') = \frac{a_d(t')}{A_d|W_0^T U_d|} \quad , \tag{54}$$

where W_0 is the steady-state weight vector that would occur without interference,

$$W_0 = (\Phi_d + \Phi_n)^{-1}S. \tag{55}$$

(Φ_d, Φ_n and S are given in (19), (21) and (23).) The results below are presented in terms of $a_{dn}(t')$ rather than $a_d(t')$ because the effect of the interference can be seen by comparing $a_{dn}(t')$ with unity.

The output desired signal power is

$$P_d(t') = (1/2)E\{|\tilde{s}_d(t')|^2\} = (1/2)A_d^2|W^T(t')U_d|^2 \quad . \tag{56}$$

The output interference signal is

$$\tilde{s}_i(t') = W^T(t')X_i = A_i a_i(t)W^T(t')U_i e^{j(\omega_0 t + \psi_i)} \tag{57}$$

and the output interference power is

$$P_i(t') = (1/2)E\{|\tilde{s}_i(t')|^2\} = (1/2)A_i^2 a_i^2(t)|W^T(t')U_i|^2 \quad . \tag{58}$$

The output thermal noise power is

$$P_n(t') = \frac{\sigma^2}{2} W^\dagger(t')W(t'). \tag{59}$$

19

From these quantities, the output interference-to-noise ratio (INR),

$$INR = \frac{P_i(t')}{P_n(t')} \qquad , \qquad (60)$$

and the output signal-to-interference-plus-noise ratio (SINR),

$$SINR = \frac{P_d(t')}{P_i(t') + P_n(t')} \qquad , \qquad (61)$$

may be computed as functions of t'.

In the next section, we present an example to illustrate the use of this technique.

III. AN EXAMPLE

Consider a modulation envelope of the form

$$a_i(t') = \frac{1}{2} (1 + \cos \omega_m' t') \qquad . \qquad (62)$$

For this $a_i(t')$, the interference is an ordinary amplitude modulated signal, as shown in Figure 2, with 100% modulation. The coefficient 1/2 in (62) is included to normalize $a_i(t')$ as in (11). The Fourier coefficients of

$$a_i^2(t') = \frac{1}{4} (1 + \cos \omega_m' t')^2 \qquad (63)$$

20

are

$$P_o = \frac{3}{8} \tag{64}$$

$$P_{\pm 1} = \frac{1}{4} \tag{65}$$

and

$$P_{\pm 2} = \frac{1}{16} \quad . \tag{66}$$

The system in (51) becomes

$$
\begin{bmatrix}
h_N + P_o & P_1 & P_2 & 0 & & 0 & 0 \cdots\cdots 0 \\
P_{-1} & h_{N-1}+ P_o & P_1 & P_2 & & 0 & 0 \cdots\cdots 0 \\
\vdots & & \vdots & \vdots & & \vdots & \vdots \\
0 \cdots\cdots P_{-2} & P_{-1} & h_o + P_o & P_1 & P_2 & 0 \cdots 0 \\
\vdots & & & & & & \\
0 & 0 \cdots\cdots\cdots\cdots\cdots 0 & P_{-2} & P_{-1} & h_{-N} + P_o
\end{bmatrix}
\begin{bmatrix}
\alpha_{N,1} \\
\alpha_{N-1,1} \\
\vdots \\
\alpha_{0,1} \\
\vdots \\
\alpha_{-N,1}
\end{bmatrix}
=
\begin{bmatrix}
0 \\
0 \\
\vdots \\
C \\
0 \\
\vdots \\
0
\end{bmatrix}
$$

$$\tag{67}$$

where C and h_n are defined in (48) and (49).

21

In general, one finds that the number of terms N needed to construct W(t') from the series (50) varies with the signal parameters. In each case, one must increase N until the first four terms on each end of the $\alpha_{n,1}$ vector in (67) are essentially zero and until the values of $\alpha_{n,1}$ for small n are not affected by further increases in N. To solve (67), we have used Gauss elimination with full pivoting [11,12] and also double precision (16 decimal places on the VAX-11/780). In initial tests of this method, the weight vector W(t') was checked in numerous cases against Runge-Kutta solutions [11,12] of (1).

As discussed above, time varying weights have two effects on array performance. They cause the array to modulate the desired signal, and they cause the array output signal-to-interference-plus-noise ratio (SINR) to vary periodically with time. In part A below, we show typical curves of desired signal modulation, output INR and SINR as functions of time. In Parts B-E, we describe the effect of each signal parameter on the desired signal modulation. In Part F, we assume the array is used in a digital communication system and describe the effect of this interference on bit error probability.

A. Typical Waveforms

Figures 3, 4 and 5 show typical curves of $a_{dn}(t')$, output INR and SINR as functions of time over one period of the modulation. These curves are for the case $\theta_d=0°$, $\theta_i=5°$, $\xi_d=10$ dB, $\xi_i=20$ dB and

22

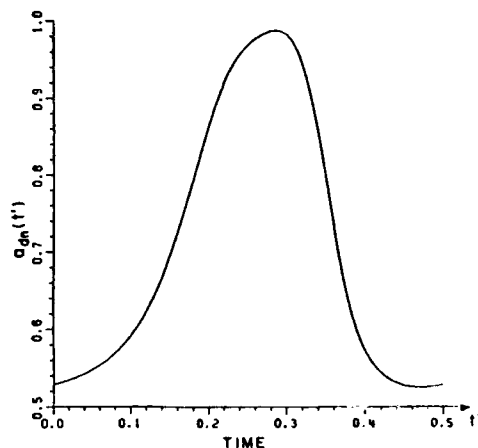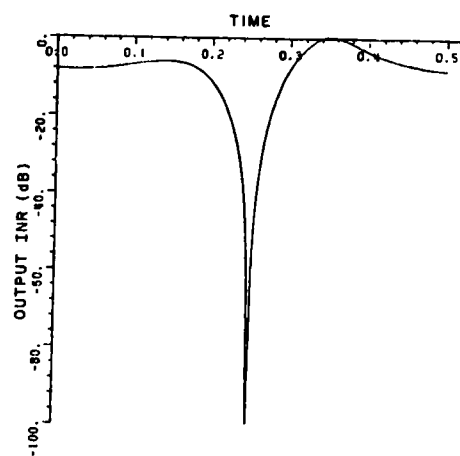Figure 3. $A_{dn}(t')$ versus time. $\theta_d=0°$, $\theta_i=5°$, $\xi_d=10$ dB. $\xi_i=20$ dB, $f_m'=2$.

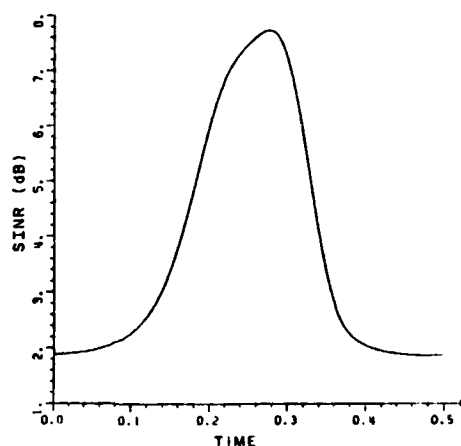Figure 4. INR versus time. $\theta_d=0°$, $\theta_i=5°$, $\xi_d=10$ dB. $\xi_i=20$ dB, $f_m'=2$.

Figure 5. SINR versus time. $\theta_d=0°$, $\theta_i=5°$, $\xi_d=10$ dB. $\xi_i=20$ dB, $f_m'=2$.

23

$f_m'=2$ (where $f_m' = \frac{\omega_m'}{2\pi}$). As may be seen, for this set of parameters, the AM interference signal produces substantial envelope modulation, and the output INR and SINR vary considerably over the modulation period.

Calculations of the phase $\eta_d(t')$ in (53), on the other hand, show that $\eta_d(t')$ is constant. The adaptive array does not produce phase modulation on the desired signal with this interference. This important result occurs for all signal parameters, not just those used in Figures 3 through 5. The same result was also found for pulsed interference [2] and for DSBSC-AM interference [3].

Figures 3 through 5 are intended merely to illustrate typical array behavior with AM interference. In general, the desired signal modulation and the SINR variation depend greatly on the choice of signal parameters θ_d, ξ_d, θ_i, ξ_i and f_m'. In Parts B-E below, we describe the effect of each signal parameter on the desired signal modulaiton. To characterize the desired signal modulation, we define three quantities. First, we let a_{max} and a_{min} be the maximum and minimum values of $a_{dn}(t')$ during the modulation period. Then we define

$$m = \frac{a_{max} - a_{min}}{a_{max}} \tag{68}$$

m is the fractional modulation on the desired signal. We shall refer to a_{max} as the envelope peak and to m as the envelope variation. In Parts B-E, we describe how m and a_{max} depend on each signal parameter.

24

B. The Effect of Angle of Arrival

Desired signal modulation is small unless θ_i is close to θ_m. When θ_i is far from θ_d, the envelope variation m is small and the peak a_{max} is close to unity. Figures 6 and 7 show typical curves of m and a_{max} as functions of θ_i for the parameters $\theta_d=0°$, $\xi_d=10$ dB and $f_m'=2$. Two curves are shown on each figure, for $\xi_i=10$ dB and 20 dB.

C. The Effect of Modulation Frequency

The variation m and the peak a_{max} are large at low f_m' and drop as f_m' increases. Figures 8 and 9 show m and a_{max} as functions of f_m' for the case $\theta_d=0°$, $\xi_d=0$ dB and $\xi_i=20$ dB.

D. The Effect of Interference-to-Noise Ratio

For low f_m', the variation m is largest at high INR. For intermediate values of f_m', m peaks at intermediate INR. a_{max} is unity for low f_m' and drops to a minimum at high f_m'. The larger the INR, the farther a_{max} drops for large f_m'. These effects may be seen in Figures 10 and 11, which show m and a_{max} for $\theta_d=0°$, $\theta_i=5°$, $\xi_d=0$ dB and for five values of ξ_i between 0 and 30 dB.

E. The Effect of Desired Signal-to-Noise Ratio

The variation m is largest and the peak a_{max} is smallest for low ξ_d. As ξ_d is increased, m decreases and a_{max} increases. Figures 12 and
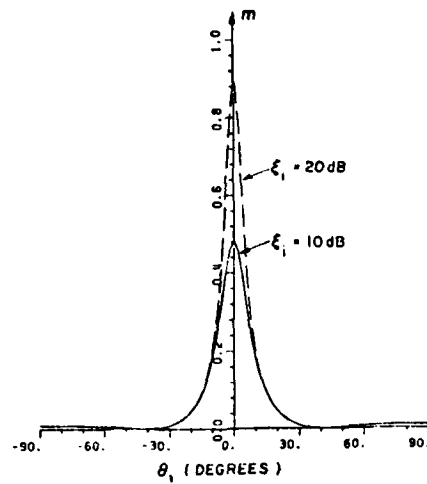
Figure 6. m versus θ_i
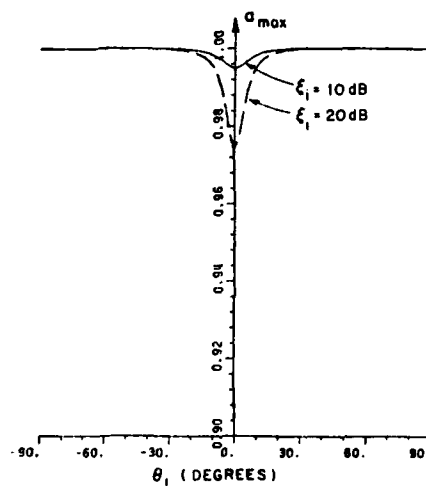
$\theta_d = 0°$, $\xi_d = 10$ dB, $f'_m = 2$.

Figure 7. a_{max} versus θ_i
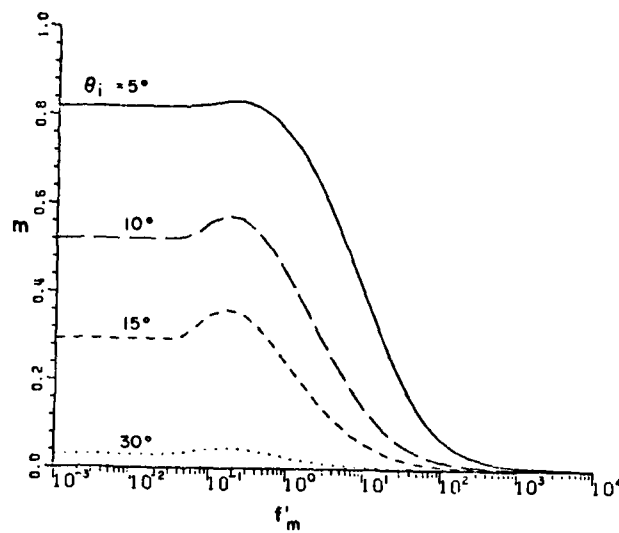
$\theta_d = 0°$, $\xi_d = 10$ dB, $f'_m = 2$.

26

Figure 8. $\underline{m \text{ versus } f'_m}$
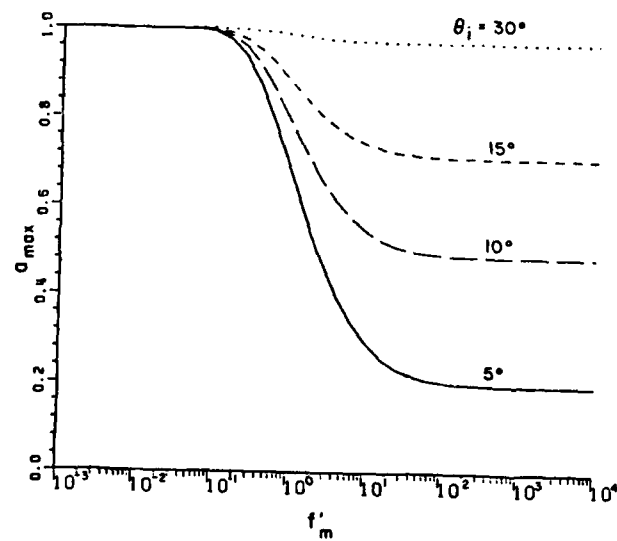
$\theta_d = 0°, \ \xi_d = 0 \text{ dB}, \ \xi_i = 20 \text{ dB}.$

Figure 9. $\underline{a_{max} \text{ versus } f'_m}$

$\theta_d = 0°, \ \xi_d = 0 \text{ dB}, \ \xi_i = 20 \text{ dB}.$

27
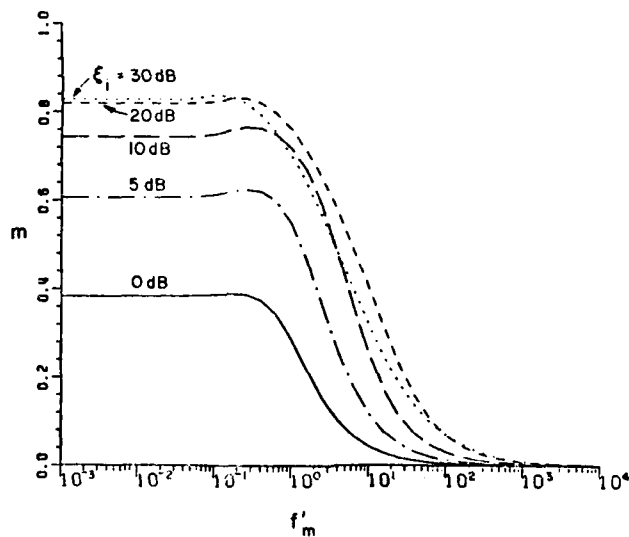
Figure 10. $\dfrac{m \text{ versus } f_m'}{\theta_d = 0°, \ \theta_i = 5°, \ \xi_d = 0 \text{ dB.}}$

Figure 11. $\dfrac{a_{max} \text{ versus } f_m'}{\theta_d = 0°, \ \theta_i = 5°, \ \xi_d = 0 \text{ dB.}}$

28
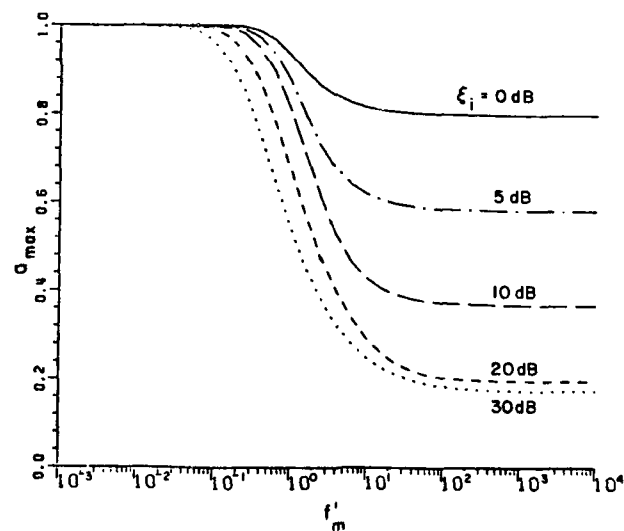
13 show m and a_{max} for $\theta_d=0°$, $\theta_i=5°$, $\xi_i=20$ dB and for four values of ξ_d between 0 and 30 dB. It is seen that for a given ξ_d, m peaks at intermediate values of f_m'.

F. Bit Error Probability

To evaluate the effect of the time-varying SINR, we assume the desired signal is a DPSK biphase modulated signal [13]. We assume the bit rate on the desired signal is much larger than the modulation frequencies in $a_i(t)$. As shown in [2,3], under these conditions we may determine the effective bit error probability $\overline{P}_e$ by averaging the instantaneous bit error probability over one period:

$$\overline{P}_e = f_m' \int_0^{1/f_m'} \frac{1}{2} e^{-SINR(t')} dt' \quad . \tag{69}$$

Figure 14 shows typical curves of $\overline{P}_e$ as a function of f_m' for $\theta_d=0°$, $\theta_i=30°$, $\xi_d=6$ dB and for several values of ξ_i between -10 dB and 30 dB. It is seen that the average bit error probability is affected very little by f_m'. It may be shown that $\overline{P}_e$ is essentially the same as that for CW interference with an INR of $(3/8)\xi_i$, i.e., with the same time-average power as the AM interference signal.
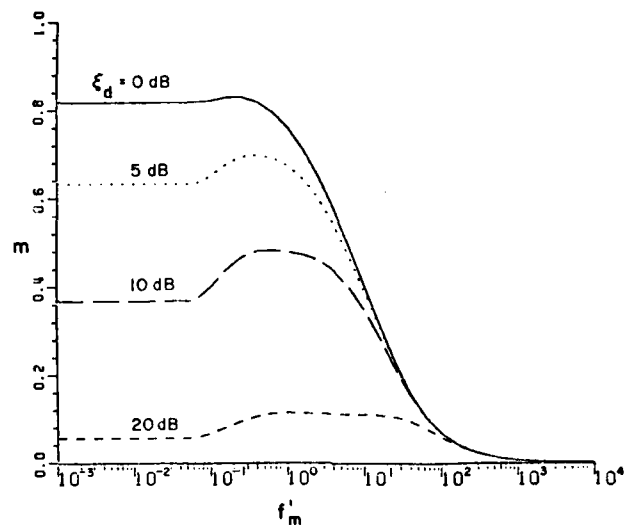
Figure 12. $\underline{m \text{ versus } f_m'}$
$\theta_d = 0°, \quad \theta_i = 5°, \quad \xi_i = 20 \text{ dB}.$
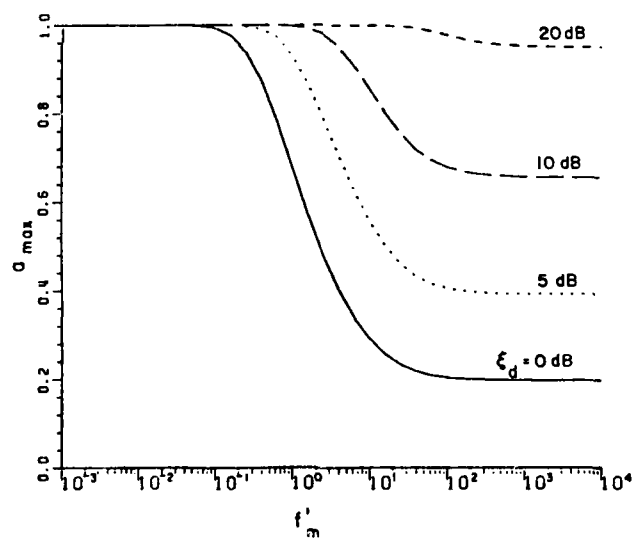
Figure 13. $\underline{a_{max} \text{ versus } f_m'}$
$\theta_d = 0°, \quad \theta_i = 5°, \quad \xi_i = 20 \text{ dB}.$

30
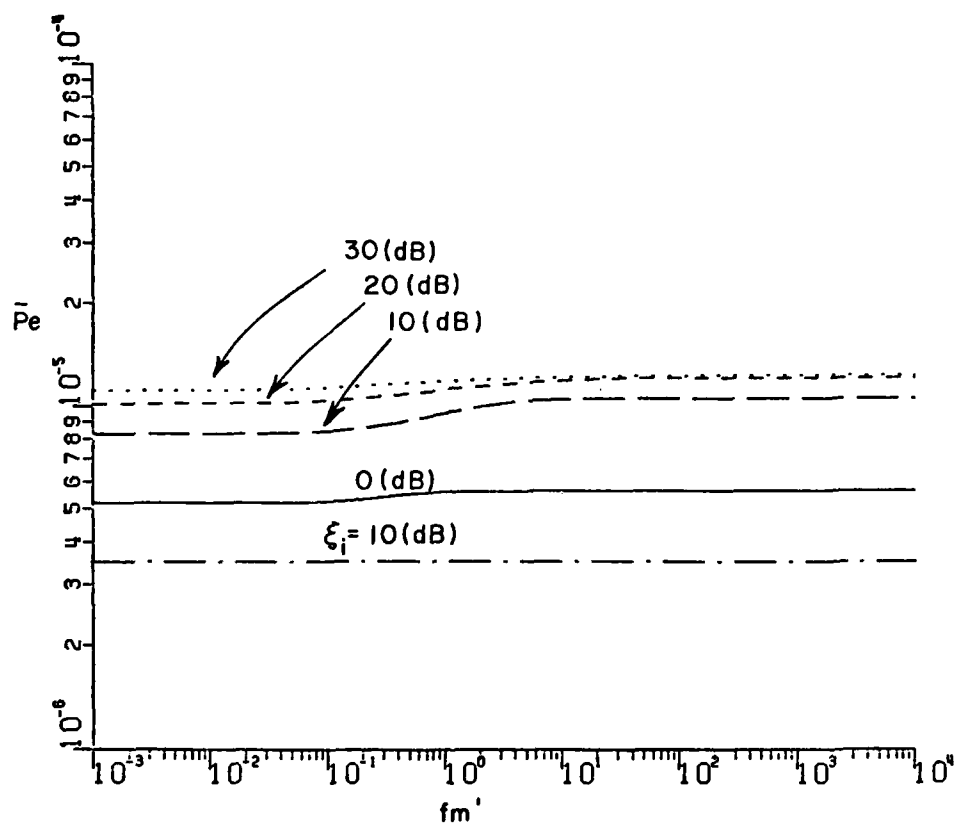
Figure 14. Bit error probability versus f_m'
$\theta_d = 0°$, $\theta_i = 30°$, $\xi_d = 6$ dB.

31

IV. SUMMARY

We have developed a mathematical technique for computing the array weights when the array is subjected to interference with periodic envelope modulation. Our approach requires that the envelope modulation be modeled with a finite number of Fourier Series terms.

To illustrate the use of this technique, we have evaluated the effects of an AM interference signal on the array. It was shown that the major effect of AM interference is to cause envelope modulation, but not phase modulation, on the desired signal. The effects of each signal parameter on desired signal modulation have been described. When the desired signal is a DPSK signal, AM interference was found to have essentially the same effect on bit error probability as CW interference. These results are similar to those obtained for DSBSC-AM interference [3].

V. REFERENCES

1. B. Widrow, P.E. Mantey, L.J. Griffiths and B.B. Goode, "Adaptive Antenna Systems", Proc. IEEE, Vol. 55, p. 2143, December 1967.

2. R.T. Compton, Jr., "The Effect of a Pulsed Interference Signal on an Adaptive Array", IEEE Trans. Aerospace and Electronic Systems, Vol. AES-18, p. 297, May 1982.

3. A.S. Al-Ruwais and R.T. Compton, Jr., "Adaptive Array Behavior with Sinusoidal Envelope Modulated Interference", accepted for publication in IEEE Transactions on Aerospace and Electronic Systems.

4. P.M. Morse and H. Feshback, Methods of Theoretical Physics, McGraw-Hill Book Co., New York, 1953; Section 5.2, p. 555ff.

5. R.L. Riegler and R.T. Compton, Jr., "An Adaptive Array for Interference Rejection", Proc. IEEE, Vol. 61, p. 748, June 1973.

6. R.T. Compton, Jr., R.J. Huff, W.G. Swarner and A.A. Ksienski, "Adaptive Arrays for Communication Systems: An Overview of Research at The Ohio State University", IEEE Trans. Antennas Propagation, Vol. AP-24, p. 599, September 1978.

7. R.T. Compton, Jr., "An Adaptive Array in a Spread Spectrum Communication System", Proc. IEEE, Vol. 66, p. 289 March 1978.

8. J.H. Winters, "Spread Spectrum in a Four-Phase Communication System Employing Adaptive Antennas", IEEE Trans. on Communications, Vol. COM-30, p. 929, May 1982.

9. H. D'Angelo, Linear Time-Varying Systems: Analysis and Synthesis, Allyn and Bacon, Boston, 1970.

10. R.S. Kennedy, Fading Dispersive Communication Channels, John Wiley and Sons, New York, 1969.

11. D.M. Young and R.T. Gregory, A Survey of Numerical Mathematics, Addison-Wesley Publishing Co., Reading, Massachusetts, 1972.

12. F.B. Hildebrand, Introduction to Numerical Analysis, McGraw-Hill Book Co., New York, 1974.

13. W.C. Lindsey and M.K. Simon, Telecommunication Systems Engineering, Prentice-Hall Inc., Englewood Cliffs, New Jersey, 1973.

4. P.M. Morse and H. Feshback, *Methods of Theoretical Physics*, McGraw-Hill Book Co., New York, 1953; Section 5.2, p. 555ff.

5. R.L. Riegler and R.T. Compton, Jr., "An Adaptive Array for Interference Rejection", Proc. IEEE, Vol. 61, p. 748, June 1973.

6. R.T. Compton, Jr., R.J. Huff, W.G. Swarner and A.A. Ksienski, "Adaptive Arrays for Communication Systems: An Overview of Research at The Ohio State University", IEEE Trans. Antennas Propagation, Vol. AP-24, p. 599, September 1978.

7. R.T. Compton, Jr., "An Adaptive Array in a Spread Spectrum Communication System", Proc. IEEE, Vol. 66, p. 289, March 1978.

8. J.H. Winters, "Spread Spectrum in a Four-Phase Communication System Employing Adaptive Antennas", IEEE Trans. on Communications, Vol. COM-30, p. 929, May 1982.

9. H. D'Angelo, *Linear Time-Varying Systems: Analysis and Synthesis*, Allyn and Bacon, Boston, 1970.

10. R.S. Kennedy, *Fading Dispersive Communication Channels*, John Wiley and Sons, New York, 1969.

11. D.M. Young and R.T. Gregory, *A Survey of Numerical Mathematics*, Addison-Wesley Publishing Co., Reading, Massachusetts, 1972.

12. F.B. Hildebrand, *Introduction to Numerical Analysis*, McGraw-Hill Book Co., New York, 1974.

13. W.C. Lindsey and M.K. Simon, *Telecommunication Systems Engineering*, Prentice-Hall Inc., Englewood Cliffs, New Jersey, 1973.

END

FILMED

5-83

DTIC